*Journal of Thermal Analysis and Calorimetry, Vol. 58 (1999) 617-623*

# THE NON-ISOTHERMAL DEVITRIFICATION OF GLASSES IN THE $SrO{\cdot}4GeO_2$–$BaO{\cdot}4GeO_2$ COMPOSITION RANGE

*M. Catauro and G. Laudisio*

Department of Materials and Production Engineering, University 'Federico II' Piazzale Tecchio, 80125 Napoli, Italy

## Abstract

The effect of replacing SrO by BaO on the glass transition temperature and on devitrification behaviour in a series of glasses in the strontium tetragermanate – barium tetragermanate composition range has been studied by differential thermal analysis, X-ray diffraction and Fourier-transform infrared spectra. All glasses studied exhibit internal crystal nucleation. The progressive replacing of SrO by BaO causes the decrease of the glass transition temperature. Solid solutions between $SrGe_4O_9$ and $BaGe_4O_9$ were found to crystallize in glass containing both SrO and BaO. The effect of the specific surface of the glass samples on devitrification processes has been also pointed out.

**Keywords:** glasses, devitrification, germanate

## Introduction

The properties of binary $M_2O$–$GeO_2$ and $MO$–$GeO_2$ glasses have been extensively studied [1–6]. Phase equilibria in the binary germanate system have been also reported [7]. On the other hand very little is known about ternary germanate glasses. This paper is part of a research program with the aim of filling this gap.

In previous papers [8–10] the effect on glass transition temperature and devitrification behavior of the progressive substitution of an alkaline oxide $M_2O$ by another $M'_2O$ oxide in tetragermanate glasses were discussed. The substitution of $M_2O$ by $M'_2O$ causes the value of the glass transition temperature to go through a minimum at molar ratio $M_2O/M'_2O$ =1 according with the 'mixed alkali effect'. The structures of all the studied glasses contain $GeO_4$, and $GeO_6$ groups in near the same molar ratio. In the lithium – sodium tetragermanate glasses a ternary compound $LiNaGe_4O_9$ was found among the crystallizing phases [8]. The stability of the lithium potassium tetragermanate glasses increases with the increase of the difference between crystallizing phases and mother glass composition [9]. In the sodium – potassium tetragermanate glasses solid solutions between $Na_4Ge_9O_{20}$ and $K_4Ge_9O_{20}$ crystallize [10]. The devitrification behaviour of ternary tetragermanate glasses containing $Ba^{2+}$ and $Pb^{2+}$ ions in 3/1, 1/1 and 1/3 molar ratios, has been also studied [11]. Glasses with 3/1 and 1/1 $Ba^{2+}/Pb^{2+}$ molar ratio are phase separated and devitrify in two steps.

*1418–2874/99/ $ 5.00*

*Akadémiai Kiadó, Budapest*
*Kluwer Academic Publishers, Dordrecht*

Bulk crystallization of $BaGe_4O_9$ is followed at higher temperatures by $GeO_2$ crystals growth on the surface of the samples. The glass with 1/3 $Ba^{2+}/Pb^{2+}$ molar ratio devitrifies into a solid solution of $BaGe_4O_9$ and $PbGe_4O_9$ crystals.

In the present work the effect of a progressive replacement of SrO by BaO, on the structure, the glass transition temperature and the devitrification behaviour of tetragermanate glasses were studied by Fourier-transform infrared spectroscopy (FTIR), differential thermal analysis (DTA) and X-ray diffraction (XRD).

## Experimental

The glass compositions are expressed by the general formula:

$$(1-x)\mathrm{SrO}\cdot x\mathrm{BaO}\cdot 4\mathrm{GeO_2}$$

with $x$=0.00; 0.25; 0.50; 0.75; 1.00. In the course of the paper each glass is named by the corresponding $x$ value. The glasses were prepared by mixing appropriate quantities of ultra pure strontium carbonate (Aldrich), barium carbonate (Aldrich) and germanium oxide (Heraeus) in a batch sized to yield 3 g of glass. The glasses were melted in an uncovered Pt crucible in an electric oven. The crucible containing the glass was weighed both before and after the glass was removed. The mass of the glass agreed with that anticipated from the batch calculation. This result indicates that the actual glass composition is close to that based on the glass batch. The melts were quenched by plunging the bottom of the crucible into cold water. Although this resulted in fracture of the glass, for all the composition pieces of transparent glass of size sufficient for the experimental measurements were obtained by this technique.

Fourier-transform infrared (FTIR) absorption spectra were recorded in the 4000–400 $cm^{-1}$ range using a Mattson 5020 system, equipped with a DTGS KBr (deuterated triglycine sulfate with potassium bromide windows) detector. A spectral resolution of 2 $cm^{-1}$ was chosen. Each test sample was mixed with KBr (1 wt.% of former) in an agate mortar, and then pressed into 200 mg pellets of 13 mm diameter. The spectrum for each sample represents an average of 20 scans, which were normalized to the spectrum of the blank KBr pellet. The FTIR spectra have been analyzed by a Mattson software (FIRST Macros).

DTA curves were recorded in air at a heating rate of 10°C $min^{-1}$ on bulk or fine powdered (<45 micron) specimens (about 50 mg) from room temperature to 900°C. A Netzsch thermoanalyser High Temperature DSC 404 was used with $A1_2O_3$ as reference material. The experimental error in DTA temperature is ±l°C. The DTA curves have been elaborated by a Netzsch software.

The amourphous nature of the glasses and the identification of the phases crystallizing in the glass during the DTA runs were ascertained by X-ray diffraction (XRD) using a Philips diffractometer. Powders of each glass sample were scanned from $2\Theta=5°$ to 60° using $CuK_\alpha$ radiation.

## Results and discussion

Figure 1 shows the DTA curves of the five as-quenched glasses recorded on bulk samples. A slope change followed by an exothermic peak occurs on all curves. The slope change may be attributed to the glass transition. In this work, the extrapolated onset of the slope change was taken, Fig. 2, as the glass transition temperature, $T_g$. The values of $T_g$ for the five investigated glasses are reported in Table 1.

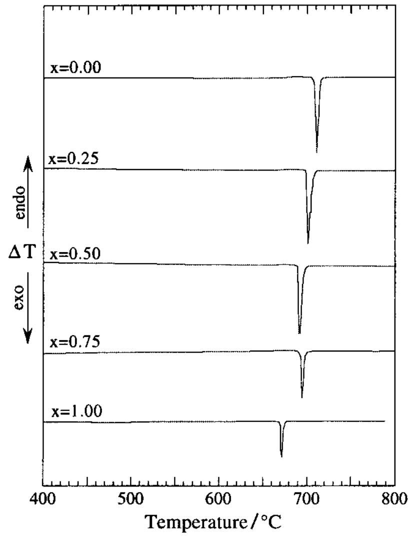

**Fig. 1** DTA curves recorded at 10°C $\text{min}^{-1}$ for glasses of composition $(1–x)\text{SrO}\cdot x\text{BaO}\cdot 4\text{GeO}_2$

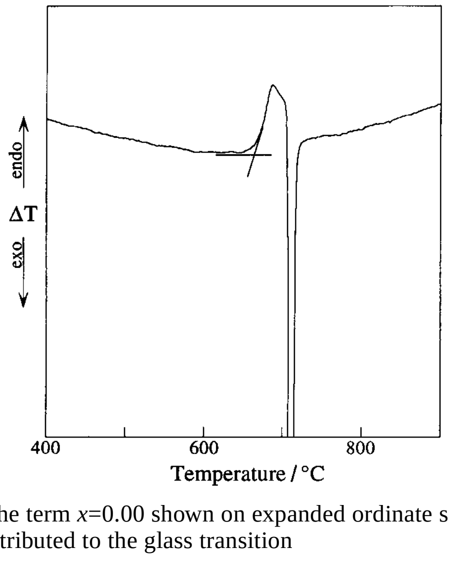

**Fig. 2** DTA curve of the term $x$=0.00 shown on expanded ordinate scale to well display the slope change attributed to the glass transition

**Table 1** DTA and IR data for glasses of composition $(1-x)SrO\cdot xBaO\cdot 4GeO_2$

| Glasses | $T_g$/°C | $T_p$/°C | $\nu_1$/cm$^{-1}$ | $\nu_2$/cm$^{-1}$ |
|---|---|---|---|---|
| $x$=0.00 | 664 | 710(707) | 756 | 577 |
| $x$=0.25 | 659 | 700(701) | 748 | 575 |
| $x$=0.50 | 653 | 691(692) | 747 | 569 |
| $x$=0.75 | 649 | 695(691) | 754 | 576 |
| $x$=1.00 | 638 | 677(675) | 754 | 569 |

$T_g$ – glass transition temperatures
$T_p$ – DTA peak temperatures of bulk samples (in brackets of powdered samples)
($\nu_1$ and $\nu_2$) – frequencies of the two strongest intensity bands in crystallized samples

According to Ray [12], the effect of any cation on $T_g$ is related to the following factors: (i) reduction in density of covalent cross-linking; (ii) change in oxygen density of the network; (iii) number and strength of the cross-links between oxygen and the cation. In the glasses studied the O/Ge ratio is constant (i.e. O/Ge=2.25) and the $GeO_4/GeO_6$ molar ratio is the same, therefore the cross link density does not change. The strength and the number of the cross-links between oxygen and the cations are related to the coordination number and to the radius and of the cations. The coordination number is 8 for both cations. The M–O strength is reduced as a result of the larger radii of $Ba^{2+}$ (0.143 nm) compared with $Sr^{2+}$ (0.127 nm). Therefore the progressive replacing of $Sr^{2+}$ by $Ba^{2+}$ causes the decrease of the glass transition temperature.

Nucleation in glass-forming systems can occur either in the volume or on the surface of the sample. In practice, surface crystal nucleation occur more easily and is observed in most compositions. To achieve internal crystal nucleation it is often necessary to add nucleating agents. However certain glass systems nucleate internally without such additions. The total number of nuclei, $N$, per unit volume is the sum of surface nuclei, $N_s$, of homogeneous bulk nuclei $N_b$ formed during the DTA run and heterogeneous bulk nuclei $N_c$ [13] . The value of $N_s$, $N_b$ and $N_c$ are proportional to the specific surface area of the samples, the reciprocal of the DTA heating rate and the amount of nucleating agent, respectively. The higher the number of $N$ is, the lower the temperature of the DTA crystallization peak is [14]. Moreover the shape of the DTA crystallization peak is strongly affected by the crystallization mechanism [15] to surface and bulk crystallization corresponds broad and sharp peaks, respectively.

In the studied glasses no nucleating agent was added ($N_c$=0). The sharp shape of the crystallization peaks on the DTA curves, carried out on bulk samples (low specific surface area), Fig. l, suggests that in all glasses studied internal crystal nucleation is dominant $N_b>>N_s$. To confirm this hypothesis DTA curves were also recorded on very fine powdered samples. No appreciable differences of the temperature, $T_p$, (Table 1) and the shape of the crystallization peak were found. Taking into account the great increase of the number of surface nuclei due to the high specific surface area of the very fine powdered samples this result indicates that the specific surface area of the samples has no influence on the devitrification process of these glasses and surface crystallization compared with bulk nucleation can be neglected.

To ascertain the amorphous nature of the glasses and to identify the phases crystallizing during the DTA runs, XRD measurements were carried out on the as-quenched glasses and on samples subjected to a DTA run from room temperature to 800°C.

The XRD patterns of the as-quenched glasses show broad humps characteristic of their amorphous state.

The XRD patterns of samples of the glasses with $x$=0.00 and $x$=1.00 exhibit, Fig. 3, several sharp reflections that were all assigned to $SrGe_4O_9$ (JCPDS file 14–29) and $BaGe_4O_9$ (JCPDS file 13–295) crystals, respectively.

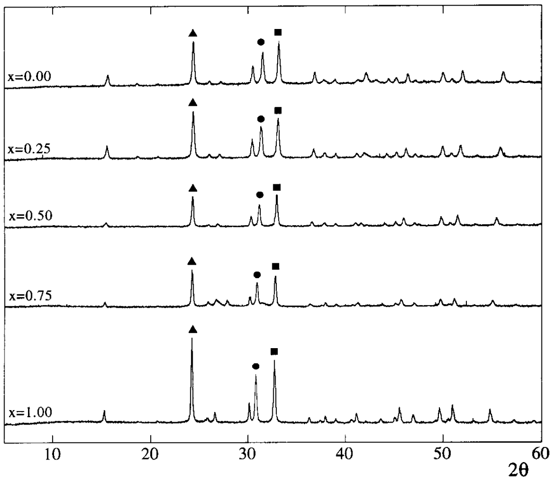

**Fig. 3** X-ray diffraction patterns for glasses of composition $(1–x)SrO·xBaO·4GeO_2$

The XRD patterns of the crystallizing phases in the intermediate terms of the series shown in Fig. 3 suggest the formation of solid solutions. Usually, the unit cell expands if a small $Sr^{2+}$ ion is being replaced by a larger $Ba^{2+}$ one. From Bragg's law and the d-spacing formulae, an increase in the unit cell parameters leads to an increase in the d-spacing of powder lines, the whole pattern shifts to lower values of 2Θ although all the lines do not usually move by the same amount. In Fig. 4 the d-spacing of the three strongest peaks detected on the XRD patterns of Fig. 3 are reported as function of $x$. The d-spacing according to Vergard's law change linearly with glass composition. In the XRD pattern of the glass $x$=0.25 the strongest reflection of $GeO_2$ crystals was also found.

Figure 5 shows the infrared percentage transmission spectra of the devitrified glasses in the 400–1200 cm$^{-1}$ range where the Ge–O–Ge and O–Ge–O stretching and deformation modes are actives. The two strongest absorption peaks lie at about 750 and 570 cm$^{-1}$.

From previous studies [4], is known that in the infrared spectra of hexagonal and vitreous $GeO_2$, in which the coordination number of germanium is 4, the absorption

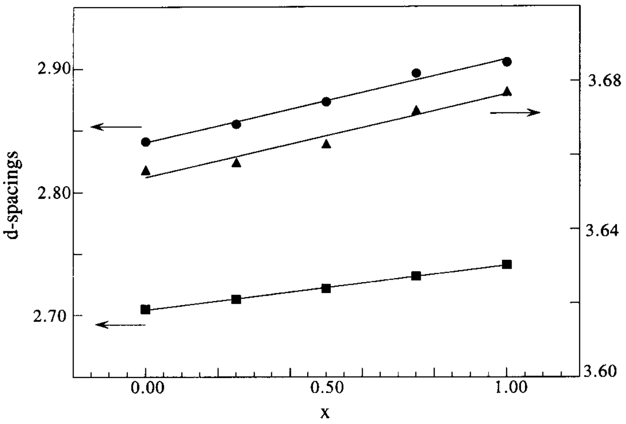

**Fig. 4** d-spacings of indexed peaks of Fig. 3 *vs*. glass composition

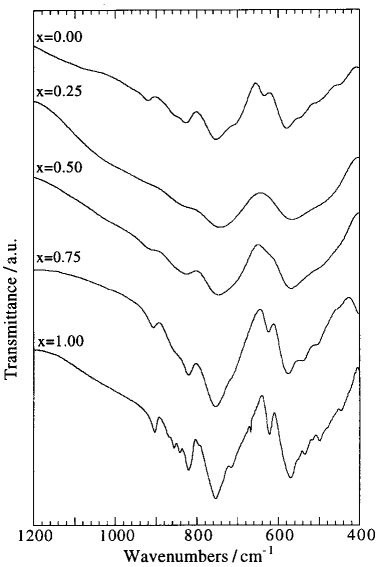

**Fig. 5** FTIR transmittance spectra for glasses of composition (1–*x*)SrO·*x*BaO·4GeO$_2$

band, due to the Ge–O–Ge stretching lies at 878 cm$^{-1}$, while in tetragonal GeO$_2$, in which germanium assumes sixfold coordination, this band occurs at 688 cm$^{-1}$. In alkali germanate the coordination number of Ge atoms changes from 4 to 6 with the addition of alkali oxide to GeO$_2$ glass and this band progressively shifts towards lower wavenumbers values [4].

The spectra of Fig. 5 exhibit near the same shift of this band as shown in Table 1. This result suggests a similar GeO$_4$/GeO$_6$ molar ratio in all the glasses of the series. The absorption band at about 550 cm$^{-1}$ may be related to mixed stretching-bending vibrations of GeO$_4$ tetrahedra [16].

## Conclusions

From the experimental results the following conclusions can be drawn:

a. The progressive replacing of SrO by BaO causes a progressive decrease of the glass transition temperature.

b. All glasses exhibit internal crystal nucleation.

c. The end members of the series $x$=0.00 and $x$=1.00 devitrified into $SrGe_4O_9$ and $BeGe_4O_9$ crystals, respectively. In the intermediate terms of the series solid solutions of $SrGe_4O_9$ and $BaGe_4O_9$ crystallized.

d. The struct ures of the devitrified glasses contain $GeO_4$ and $GeO_6$ in the same molar ratio.

## References

1 K. S. Evstropiev and A. O. Iivanov, Advances in glass technology, Part 2 Ed. F. R. Matson and G. E. Rindone. Plenum Press, New York 1963, p. 79.
2 M. K. Murthy and J. Ip, Nature, Lond. 201 (1964) 3285.
3 J. E. Shelby, J. Am. Ceram. Soc., 57 (1974) 436.
4 M. K. Murthy and E. M. Kirby, Physics Chem. Glasses, 5 (1964) 144.
5 S. Sakka and K. Kamiya, J. Non-Cryst. Solids, 49 (1982) 103.
6 H. Verweij and J. H. J. M. Buster, J. Non-Cryst. Solids, 34 (1979) 81.
7 E. M. Levin, C. R. Robins and H. C. McMurdie, Phase diagrams for ceramists, American Ceramic Society, Columbus, Ohio 1964, p.93.
8 M. Catauro, A. Aronne, P. Pernice and A. Marotta, J. Mater. Sci. Letters, 15 (1996) 817.
9 G. Laudisio and M. Catauro, J. Europ. Cer. Soc., 18 (1998) 359.
10 G. Laudisio and M. Catauro, Mater. Chem. Phys., 51 (1997) 54.
11 G. Laudisio and M. Catauro, Physics Chem. Glasses, 39 (1998) 62.
12 N. H. Ray, J. Non-Cryst. Solids, 15 (1974) 423.
13 A. Marotta, A. Buri and F. Branda, Thermochim. Acta, 40 (1980) 397.
14 A. Marotta, A. Buri and F. Branda, J. Mater. Sci., l6 (1981) 341.
15 W. W. Wendlandt in Thermal Analysis, John Wiley & Sons, 1986, p. 448.
16 K. E. Lipinska-Kalita, J. Non-Cryst. Solids, 119 (1990) 41.